P-Map: An Intuitive Plot to Visualize, Understand, and Compare Variable-Gain PI Controllers

Dongrui Wu

Industrial Artificial Intelligence Laboratory
GE Global Research, Niskayuna, NY 12309 USA
wud@ge.com

Abstract. This paper introduces P-map, an intuitive plot to visualize, understand and compare variable-gain PI controllers. The idea is to represent the difference between a target controller and a baseline controller (or a second controller for comparison) by an equivalent proportional controller. By visualizing the value of the proportional gain and examining how it changes with inputs, it is possible to qualitatively understand the characteristics of a complex variable-gain PI controller. Examples demonstrate that P-map gives more useful information than control surface for variable-gain PI controllers. So, it can be used to supplement or even replace the control surface.

Keywords: Adaptive control, control surface, fuzzy logic control, gain-scheduling control, interval type-2 fuzzy logic control, P-map, PI control, variable-gain controller.

1 Introduction

Proportional-integral-derivative (PID) control [2] is by far the most widely used control algorithm in practice, e.g., according to a survey [7] of over 11000 controllers in the refining, chemicals and pulp and paper industries, 97% of regulatory controllers are PID controllers. Among them, most are proportional-integral (PI) controllers. The input-output relation for an ideal PI controller with constant gains is

$$u(t) = k_p e(t) + k_i \int_0^t e(\tau) d\tau \tag{1}$$

where the control signal is the sum of the proportional and integral terms. The controller parameters are the constant proportional gain k_p and the constant integral gain k_i. For simplicity in the following we will use $e_i(t)$ to denote $\int_0^t e(\tau)d\tau$.

The properties of constant-gain PID controllers have been extensively studied in the literature [2, 4]. However, in practice the parameters of the system being controlled may be slowly time-varying or uncertain. For example, as an aircraft flies, its mass slowly decreases as a result of fuel consumption. In these cases, a

M. Kamel et al. (Eds.): AIS 2011, LNAI 6752, pp. 189–198, 2011.

variable-gain controller, whose gains are different at different operational conditions, may be preferred over a constant-gain controller. This is the motivation of gain scheduling control [1, 8, 11], or more generally, adaptive control [3, 18]. The input-output relation for a variable-gain PI controller may be expressed as

$$u(t) = k_p(e(t), e_i(t)) \cdot e(t) + k_i(e(t), e_i(t)) \cdot e_i(t) \tag{2}$$

In this paper we assume the variable gains k_p and k_i are functions of $e(t)$ and $e_i(t)$ only. However, the P-map method can also be applied when k_p and k_i involve other variables.

Fuzzy logic systems [5, 9, 12, 14, 16, 19], especially the TSK model [15, 17, 19, 22, 23], are frequently used to implement PI controllers. Except in very special cases [15], a fuzzy logic controller (FLC) implements a variable-gain PI control law, where the gains $k_p(e(t), e_i(t))$ and $k_i(e(t), e_i(t))$ change with the inputs. Frequently people use optimization algorithms to tune the parameters of the FLCs [6, 13, 22, 23]. Though the resulting FLCs usually have good performance, it is difficult to understand their characteristics and hence how the performance is achieved.

Traditionally people use control surface to visualize the relationship between $u(t)$ and its inputs, $e(t)$ and $e_i(t)$. An exemplar control surface is shown in the bottom left part of Fig. 1. However, the control surface only gives the user some rough ideas about the controller, e.g., complexity, continuity, smoothness, monotonicity, etc. It is difficult to estimate the control performance from only the control surface. On the other hand, the control systems literature [2, 4] has qualitatively documented the relationship between control performance and PI gains. So, it would be easier to estimate the control performance of a variable-gain PI controller if we can visualize the change of the PI gains with respect to the inputs. This paper proposes such a visualization method called P-map and illustrates how to use it to understand the characteristics of an FLC and to compare the difference between type-1 (T1) and interval type-2 (IT2) FLCs. Examples show that P-map can be used to supplement or even replace the control surface.

The rest of this paper is organized as follows: Section 2 presents the theory on P-map. Section 3 provides illustrative examples on how to use P-map to understand the characteristics of an FLC and to compare the difference between two FLCs. Finally, Section 4 draws conclusions.

2 P-Map: Theory

The effects of changing a proportional gain or an integral gain individually in a PI or PID controller is well-known in the literature [2, 4]. Generally, a larger k_p typically means faster response and shorter rising time, but an excessively large k_p may also lead to larger overshoot, longer settling time, and potential oscillations and process instability. A larger k_i implies steady state errors are eliminated more quickly; however, there may be larger overshoot.

However, if k_p and k_i are varied simultaneously, then their effects are intercorrelated and it is difficult to predict the control performance. So, if we can represent a variable-gain PI controller by a proportional controller only, then it is much easier to understand its characteristics. This is the essential idea of P-map, which is a method to understand the characteristics of a variable-gain PI controller or to compare the difference of two PI controllers using an equivalent proportional gain k_p.

To construct the P-map, we first need to identify a baseline controller for comparison. Next we introduce two methods to obtain the baseline controller, depending on the context of application.

2.1 P-Map for Understanding a Variable-Gain PI Controller

To use P-map for understanding a variable-gain PI controller $u(t)$, we need to construct a baseline constant-gain PI controller

$$u_0(t) = k_{p,0}e(t) + k_{i,0}e_i(t) \tag{3}$$

from $u(t)$. There may be different ways to construct $k_{p,0}$ and $k_{i,0}$. In this paper we use a least squares approach to fit a plane for $u(t)$: we first obtain n samples $\{e(t), e_i(t), u(t)\}$ from the controller $u(t)$, and then use the least squares method to fit a linear model

$$u(t) = k_{p,0}e(t) + k_{i,0}e_i(t) + \epsilon(e(t), e_i(t)) \tag{4}$$

Clearly,

$$u(t) = u_0(t) + \epsilon(e(t), e_i(t)) \tag{5}$$

where $\epsilon(e(t), e_i(t))$ is the difference (residual) between the variable-gain PI controller and the baseline constant-gain PI controller. $\epsilon(e(t), e_i(t))$ can be visualized by the difference between the control surfaces of $u(t)$ and $u_0(t)$, as shown in the bottom left part of Fig. 2.

P-map is used to better visualize and understand the effect of $\epsilon(e(t), e_i(t))$. As the relationship between the proportional gain and the performance of a PI controller is well-known, we want to represent $\epsilon(e(t), e_i(t))$ by a variable-gain proportional controller, i.e.,

$$\epsilon(e(t), e_i(t)) = k'_p(e(t), e_i(t)) \cdot e(t) \tag{6}$$

In other words, the proportional gain in the P-map is computed as

$$k'_p(e(t), e_i(t)) = \frac{\epsilon(e(t), e_i(t))}{e(t)} \tag{7}$$

P-map is then used to visualize how $k'_p(e(t), e_i(t))$ changes with $e(t)$ and $e_i(t)$ and hence to understand the characteristics of the variable-gain PI controller. Two illustrative examples are shown in Section 3.

2.2 P-Map for Comparing Two PI Controllers

To use P-map for comparing a variable-gain PI controller $u_2(t)$ against another PI controller $u_1(t)$, $u_1(t)$ is used as the baseline controller. We then compute the difference between $u_2(t)$ and $u_1(t)$, i.e.,

$$\epsilon(e(t), e_i(t)) = u_2(t) - u_1(t) \tag{8}$$

$\epsilon(e(t), e_i(t))$ can be visualized by the difference between the control surfaces of $u_2(t)$ and $u_1(t)$, as shown in the left part of Fig. 3. However, P-map is a better visualization method, as demonstrated in the next section. The proportional gain in the P-map is again computed by (7). An example will be shown in Section 3.

2.3 Discussions

Observe from (7) that the equivalent gain $k'_p(e(t), e_i(t))$ cannot be computed when $e(t)$ equals 0, and also there may be numerical instabilities when $|e(t)|$ is very close to 0. This is a limitation of the P-map. However, it only concerns with a very small area in the P-map and does not affect the global understanding of the characteristics of a controller.

In this section we have introduced P-map for variable-gain PI controllers. However, P-map can also be applied to variable-gain proportional and PD controllers. For variable-gain proportional controllers, the P-map becomes a curve instead of a plane. P-map can also be computed for PID controllers; however, for visualization we need to plot the P-map in 4-dimensional space, which is difficult. But this is not a unique limitation for the P-map because we have difficulty plotting the control surface of a PID controller in 4-dimensional space too. If a good visualization method for the control surface of a PID controller can be developed, then it can be applied to the P-map, too, and the advantages of the P-map over the control surface can again be demonstrated.

In practice we may implement a PI controller as [10, 22, 23]

$$\dot{u}(t) = k_p(\dot{e}(t), e(t)) \cdot \dot{e}(t) + k_i(\dot{e}(t), e(t)) \cdot e(t) \tag{9}$$

where $\dot{u}(t)$ is the change in control signal, and $\dot{e}(t)$ is the change in feedback error. For this implementation we compute the proportional gain in P-map as

$$k'_p(\dot{e}(t), e(t)) = \frac{\epsilon(\dot{e}(t), e(t))}{\dot{e}(t)} \tag{10}$$

where $\epsilon(\dot{e}(t), e(t))$ is the difference between the control surfaces of a variable-gain PI controller and a baseline controller.

3 P-Map: Examples

In this section we show how P-map can be used for understanding the characteristics of FLCs and also comparing difference FLCs. First, the realization of the FLCs is introduced.

3.1 Configurations of the FLCs

In this section fuzzy PI controllers are realized in the form of (9). A typical rulebase may include rules in the form of

$$\text{IF } \dot{e}(t) \text{ is } \dot{E}_n \text{ and } e(t) \text{ is } E_n, \text{Then } \dot{u}(t) \text{ is } y_n \tag{11}$$

where $\dot{E}_n$ and E_n are fuzzy sets, and y_n is a crisp number.

3.2 Example 1: Constant-Gain T1 Fuzzy PI Controller

A T1 FLC with rules in (11) implements the constant-gain PI controller in (9) if [15]:

1. Triangular T1 FSs are used for input membership function (MFs) $\dot{E}_i$ and E_i, and they are constructed in such a way that for any input the firing levels of all MFs add to 1; and,
2. The consequents of the rules are crisp numbers defined as

$$y_n = k_p \dot{e}_n + k_i e_n \tag{12}$$

where $\dot{e}_n$ and e_n are apexes of the antecedent T1 MFs.

An example of such a T1 FLC is shown in the first row of Fig. 1. The apexes of both $\dot{E}_1$ and E_1 are at -1, and the apexes of both $\dot{E}_2$ and E_2 are at 1. The four rules are:

$$\begin{aligned}
&\text{IF } \dot{e}(t) \text{ is } \dot{E}_1 \text{ and } e(t) \text{ is } E_1, \text{Then } \dot{u}(t) \text{ is } -k_p - k_i \\
&\text{IF } \dot{e}(t) \text{ is } \dot{E}_1 \text{ and } e(t) \text{ is } E_2, \text{Then } \dot{u}(t) \text{ is } -k_p + k_i \\
&\text{IF } \dot{e}(t) \text{ is } \dot{E}_2 \text{ and } e(t) \text{ is } E_1, \text{Then } \dot{u}(t) \text{ is } k_p - k_i \\
&\text{IF } \dot{e}(t) \text{ is } \dot{E}_2 \text{ and } e(t) \text{ is } E_2, \text{Then } \dot{u}(t) \text{ is } k_p + k_i
\end{aligned}$$

$k_p = 2.086$ and $k_i = 0.2063$ are used in this example, and the rulebase is given in Table 1.

Table 1. Rulebase and consequents of the T1 FLC shown in Fig. 1.

$\dot{e}(t)$ \ $e(t)$	E_1	E_2
$\dot{E}_1$	-2.2923	-1.8797
$\dot{E}_2$	1.8797	2.2923

The control surface of the constant gain T1 fuzzy PI controller is shown in the bottom left part of Fig. 1. Observe that it is perfectly linear, as suggested by the theoretical results in [15]. The corresponding P-map is shown in the bottom

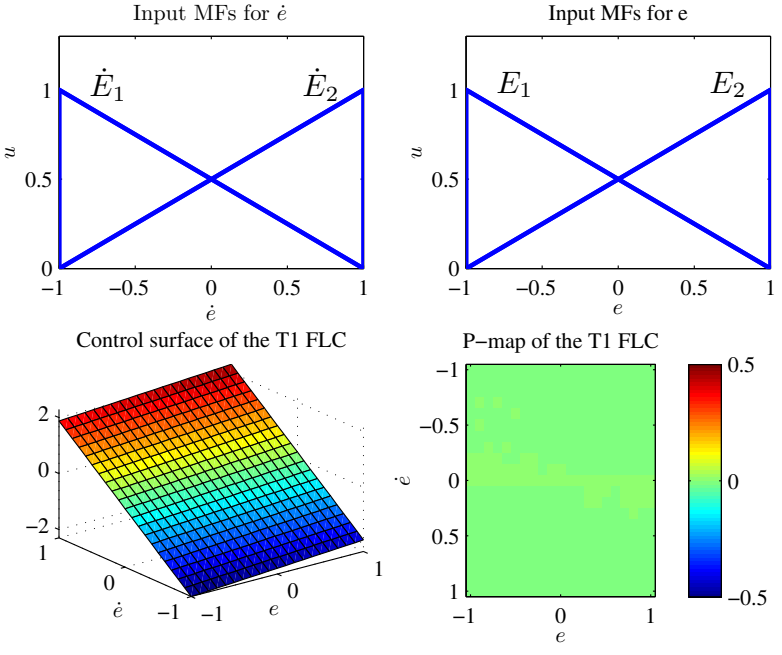

Fig. 1. MFs, control surface, and P-map for the constant-gain T1 FLC in Example 1.

right part of Fig. 1. The least squares method found the baseline constant-gain PI controller to be $\dot{u}_0(t) = 2.086\dot{e}(t) + 0.2063e(t)$, identical to the T1 FLC. As a result, $k_p'(\dot{e}(t), e(t)) = 0$ for $\forall\dot{e}(t)$ and $\forall e(t)$, as indicated in the P-map. So, both the control surface and the P-map show that the T1 fuzzy PI controller is linear.

In summary, the control surface and the P-map are equally good at showing the characteristics of linear PI controllers.

3.3 Example 2: Variable-Gain IT2 Fuzzy PI Controller

In this example, a variable-gain IT2 fuzzy PI controller is obtained from the constant-gain T1 fuzzy PI controller in Example 1 by introducing footprint of uncertainties (FOUs) [14, 22] to the T1 MFs, as shown in the first row of Fig. 2. For simplicity symmetrical FOUs are used, and the four IT2 FSs have the same amount of FOU. The corresponding rulebase is shown in Table 2. Observe that it is essentially the same as the rulebase in Table 1, except that IT2 FSs are used to replace the T1 FSs in Example 1.

Observe from the bottom left part of Fig. 2 that the control surface of the variable-gain IT2 FLC is nonlinear and non-monotonic. However, it is difficult to infer the performance of the IT2 FLC from it. To construct the P-map, the baseline PI controller was found to be $\dot{u}_0(t) = 1.2001\dot{e}(t) + 0.1602e(t)$, and the

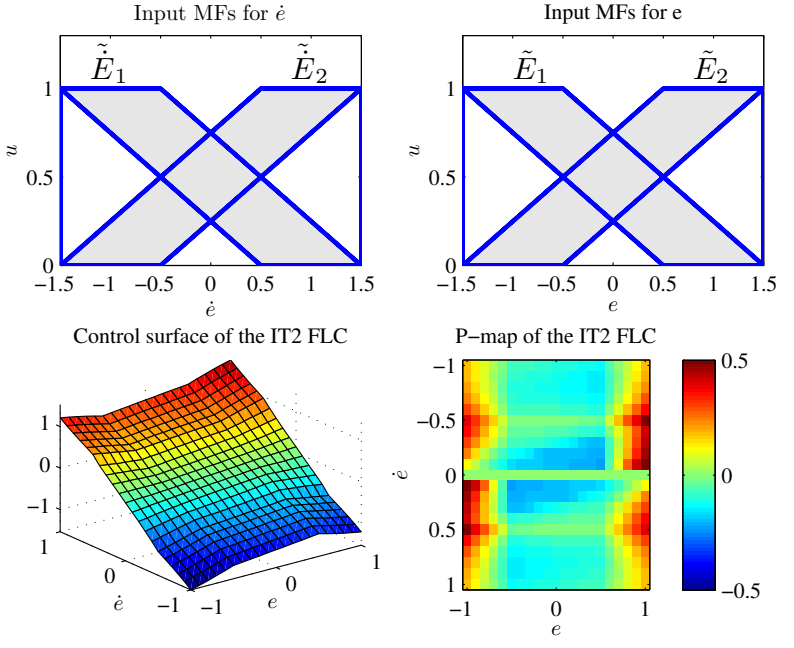

Fig. 2. MFs, control surface, and P-map for the variable-gain IT2 FLC in Example 2

corresponding P-map is shown in the bottom right part of Fig. 2. Notice that both k_p and k_i in the baseline PI controller are smaller than those in Example 1, which confirmed the finding in [24], i.e., generally introducing FOUs to a T1 FLC results a slower IT2 FLC. Observe also from the P-map that:

1. The IT2 fuzzy PI controller is nonlinear, as the proportional gain in the P-map is not a constant. However, unlike the control surface, it is difficult to observe from the P-map whether the control law is monotonic. But this is not important as the monotonicity of a controller is not used very often in control practice.
2. When $|\dot{e}(t)| \to 0$ and $|e(t)| \to 0$, $k'_p(\dot{e}(t), e(t)) < 0$, i.e., compared with the baseline linear controller $\dot{u}_0(t) = 1.2001\dot{e}(t) + 0.1602e(t)$, the IT2 FLC has a smaller proportional gain near the steady-state; so, it implements a gentler control law near the steady-state, which helps eliminate oscillations. This is difficult to be observed from the control surface.
3. When $|e(t)|$ becomes large, $k'_p(\dot{e}(t), e(t))$ increases. So, compared with the baseline linear controller $\dot{u}_0(t) = 1.2001\dot{e}(t) + 0.1602e(t)$, the IT2 FLC has a larger proportional gain when the error is large. Consequently, it implements a faster control law when the current plant state is far away from the set-point, which helps reduce rising time. Again, this is difficult to be observed from the control surface.

In summary, in this example the P-map gives us more useful information about the characteristics of the IT2 FLC than the control surface.

Table 2. Rulebase and consequents of the IT2 FLC shown in Fig. 2.

$\dot{e}(t)$ \ $e(t)$	$\tilde{E}_1$	$\tilde{E}_2$
$\tilde{\dot{E}}_1$	-2.2923	-1.8797
$\tilde{\dot{E}}_2$	1.8797	2.2923

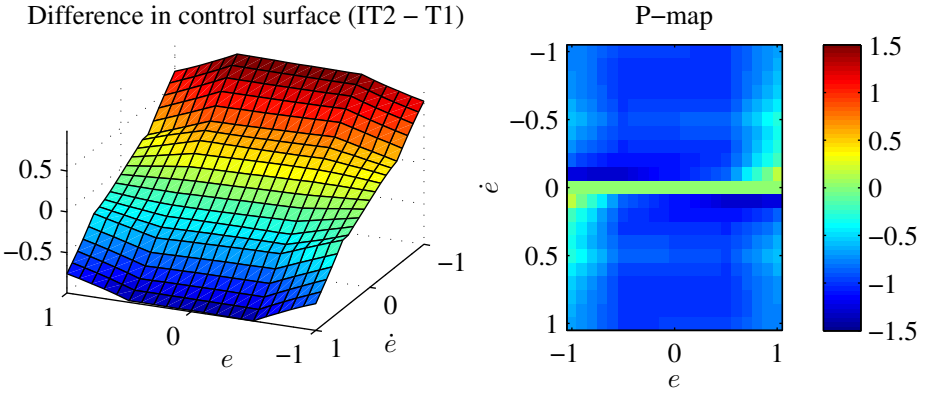

Fig. 3. Difference between the two control surfaces in Examples 2 and 1, and the corresponding P-map

3.4 Example 3: Comparing Two Fuzzy PI controllers

T1 and IT2 FLCs are fundamentally different. In [21] we showed that an IT2 FLC can output control signals that cannot be implemented by a T1 FLC. In [20] we further showed that an IT2 FLC cannot be implemented by traditionally T1 FLCs. In [24] we derived the closed-form equivalent PI gains of the IT2 FLC introduced in Example 2 for the input domain near the steady-state ($|e(t)| \to 0$ and $|\dot{e}(t)| \to 0$), and we observed that the equivalent PI gains are smaller than those in the baseline T1 FLC in Example 1; however, it is difficult to perform similar analysis for input domains far away from the steady-state.

In this example we show how P-map can be used to quantitatively compare the two FLCs in Examples 1 and 2 in the entire input domain. First we show the difference between the IT2 FLC control surface and the T1 FLC control surface in the left part of Fig. 3. We can observe that the difference is nonlinear and non-monotonic, but it is difficult to discover other useful information. However, from the P-map in the right part of Fig. 3, we can observe that[1]:

[1] Note that the following observations are specific for the T1 FLC introduced in Example 1 and the IT2 FLC introduced in Example 2. They may not be generic for all T1 and IT2 FLCs. However, for each new pair of T1 and IT2 FLCs, we can always use the P-map to discover their specific differences.

1. The difference is nonlinear, as the proportional gain in the P-map is not a constant.
2. Most part of the P-map is smaller than zero; so, generally the IT2 FLC introduced in Example 2 has a smaller proportional gain than the T1 FLC introduced in Example 1. This may result in less oscillation, but also slower response.
3. When $|e(t)|$ gets larger, the value in P-map approaches 0, i.e., the difference between the IT2 FLC and the T1 FLC becomes smaller.

In summary, in this example the P-map gives us more useful information about the difference between the two FLCs than the control surface.

4 Conclusions

In this paper we have introduced P-map, which is an intuitive plot to visualize, understand and compare variable-gain PI controllers. The idea is to represent the difference between a target PI controller and a baseline PI controller (or a second PI controller for comparison) using an equivalent proportional controller. By visualizing the value of the proportional gain and examining how it changes with inputs, we can qualitatively understand the characteristics of a complex variable-gain PI controller. As demonstrated by three examples, P-map gives more useful information than control surface for variable-gain PI controllers. So, it can be used to supplement or even replace control surface.

References

1. Apkarian, P., Adams, R.J.: Advanced gain-scheduling techniques for uncertain systems. IEEE Trans. on Control Systems Technology 6(1), 21–32 (1998)
2. Astrom, K.J., Murray, R.M.: Feedback Systems. Princeton University Press, Princeton (2008)
3. Astrom, K.J., Wittenmark, B.: Adaptive Control, 2nd edn. Addison-Wesley Longman Publishing Co., Inc., Boston (1994)
4. Astrom, K., Hagglund, T.: Advanced PID Control. ISA Press (2006)
5. Bonivento, C., Rovatti, R., Fantuzzi, C.: Fuzzy Logic Control: Advances in Methodology. In: Proc. Int'l Summer School, Ferrara, Italy (16-20, 1998)
6. Cazarez-Castro, N.R., Aguilar, L.T., Castillo, O.: Fuzzy logic control with genetic membership function parameters optimization for the output regulation of a servomechanism with nonlinear backlash. Journal of Expert Systems with Applications 37(6), 4368–4378 (2010)
7. Desborough, L., Miller, R.: Increasing customer value of industrial control performance monitoringhoneywells experience. In: Proc. 6th Int. Conf. on Chemical Process Control, Tucson, AZ, pp. 172–192 (2001)
8. Driankov, D.: Fuzzy gain scheduling. In: Bonivento, C., Fantuzzi, C., Rovatti, R. (eds.) Fuzzy Logic Control: Advances in Methodology, pp. 111–148. World Scientific, Singapore (1998)
9. Driankov, J., Hellendoorn, H., Reinfrant, M.: An Introduction to Fuzzy Control. Prentice-Hall, NY (1993)

10. Du, X., Ying, H.: Derivation and analysis of the analytical structures of the interval type-2 fuzzy-PI and PD controllers. IEEE Trans. on Fuzzy Systems 18(4), 802–814 (2010)
11. Filev, D.P.: Gain scheduling based control of a class of TSK systems. In: Farinwata, S.S., Filev, D., Langari, R. (eds.) Fuzzy Control: Synthesis and Analysis, ch. 16, pp. 321–334. John Wiley & Sons, Chichester (2000)
12. Lee, C.: Fuzzy logic in control systems: Fuzzy logic controller — Part II. IEEE Trans. on Systems, Man, and Cybernetics 20(2), 419–435 (1990)
13. Martinez-Marroquin, R., Castillo, O., Aguilar, L.T.: Optimization of interval type-2 fuzzy logic controllers for a perturbed autonomous wheeled mobile robot using genetic algorithms. Information Sciences 179(13), 2158–2174 (2009)
14. Mendel, J.M.: Uncertain Rule-Based Fuzzy Logic Systems: Introduction and New Directions. Prentice-Hall, Upper Saddle River (2001)
15. Mizumoto, M.: Realization of PID controls by fuzzy control methods. Fuzzy Sets and Systems 70, 171–182 (1995)
16. Passino, K.M., Yurkovich, S.: Fuzzy Control. Addison Wesley Longman, Inc., Menlo Park (1998)
17. Wang, L.X.: Stable adaptive fuzzy control of nonlinear systems. IEEE Trans. On Fuzzy Systems 1(2), 146–155 (1993)
18. Wang, L.X.: Adaptive Fuzzy Systems and Control: Design and Stability Analysis. Prentice Hall, Englewood Cliffs (1994)
19. Wang, L.X.: A Course in Fuzzy Systems and Control. Prentice Hall, Upper Saddle River (1997)
20. Wu, D.: An interval type-2 fuzzy logic system cannot be implemented by traditional type-1 fuzzy logic systems. In: Proc. World Conference on Soft Computing, San Francisco, CA (May 2011)
21. Wu, D., Tan, W.W.: Type-2 FLS modeling capability analysis. In: Proc. IEEE Int'l Conf. on Fuzzy Systems, Reno, NV, pp. 242–247 (May 2005)
22. Wu, D., Tan, W.W.: Genetic learning and performance evaluation of type-2 fuzzy logic controllers. Engineering Applications of Artificial Intelligence 19(8), 829–841 (2006)
23. Wu, D., Tan, W.W.: A simplified type-2 fuzzy controller for real-time control. ISA Transactions 15(4), 503–516 (2006)
24. Wu, D., Tan, W.W.: Interval type-2 fuzzy PI controllers:Why they are more robust. In: Proc. IEEE Int'l. Conf. on Granular Computing, San Jose, CA, pp. 802–807 (August 2010)